Hindawi

Research Article

Statistical Analysis for the Detection of Change Points and the Evaluation of Monthly Mean Temperature Trends of the Moulouya Basin (Morocco)

Rachid Addou [ID]**,[1] Khalid Obda,[1] Nir Y. Krakauer** [ID]**,[2,3] Mohamed Hanchane,[4] Ridouane Kessabi** [ID]**,[4] Bouchta El Khazzan,[4] and Imad Eddine Achir[4]**

[1]*Department of Geography, FLSH Sais, University Sidi Mohamed Ben Abdallah, Fez 30050, Morocco*
[2]*Department of Civil Engineering, The City College of New York, New York, NY 10031, USA*
[3]*Department of Earth and Environmental Sciences, City University of New York Graduate Center, New York, NY 10016, USA*
[4]*Department of Geography, Laboratoire Territoire Patrimoine et Histoire, FLSH Dhar El-Mehraz, Sidi Mohamed Ben Abdellah University, Fez 30050, Morocco*

Correspondence should be addressed to Nir Y. Krakauer; nkrakauer@ccny.cuny.edu

This study examines the spatiotemporal variability of mean monthly temperature in the Moulouya watershed of northeastern Morocco, highlighting associated trends. To this end, statistical methods widely recommended by climate researchers were adopted. We used monthly mean temperature data for the period 1980–2020 from 9 measuring stations belonging to the Moulouya Watershed Agency (ABHM). These stations were rigorously selected, taking into account their reliability, the length of their records, and their geographical position in the basin. In addition, a quality test and homogenization of the temperature series were carried out using the Climatol tool. The results obtained show a significant upward trend in mean monthly temperature, mainly pronounced during the summer months, in the Moulouya watershed. In fact, Z values generally exceeded the 0.05 significance level at all stations during April, May, June, July, August, and October. According to the results of Sen's slope test, mean monthly temperatures show an annual increase ranging from 0 to 0.13°C. The maximum magnitude of warming is recorded in July, specifically at Oujda Station. On an overall watershed scale, May, August, and July show a rapid warming trend, with average rates of 0.093, 0.086, and 0.08°C per year, respectively. By contrast, the series for the other months show no significant trend. Significant trend change points were also identified at watershed and station scales, mainly around 2000, primarily for accelerated warming of the summer months.

1. Introduction

Various reports by the Intergovernmental Panel on Climate Change (IPCC) predict that the increase in greenhouse gas emissions has led to a remarkable rise in global temperature. Since 1900, global surface temperatures have already risen by 1.1°C, a phenomenon unequivocally caused by human activities and primarily by greenhouse gas emissions. The temperature rise is greater on land (1.59°C) than on the sea (0.88°C) [1]. Mudelsee discussed that the application of the most modern statistical methods to the GISTEMP time series of global surface temperature reveals accelerated warming since 1974 [2]. Hansen et al. showed that global temperature rose as rapidly in the decade 2000–2010 as in the previous two decades, and the record of 12-month global mean temperature for the period covered by instrumental data was reached in 2010 [3].

Furthermore, changes in global surface temperature have been used as a major indicator of global climate change [4, 5]. Change in climate variables, including temperature, is not uniform on a global scale, and large-scale spatial and

temporal variations may exist in climatically diverse regions [6].

Local climate change is due to a number of factors, such as urban expansion partly caused by rapid population growth rates and the migration of rural populations to urban areas, all of which represent a major challenge for managers and also contribute via greenhouse gas emissions and loss of natural vegetation to the worsening of global warming and consequent rise in global temperature [7].

While understanding climate change has become a key issue in many scientific fields [8–10], knowledge of air temperature and its variability/trend is crucial to the various areas of decision-making by public managers. This knowledge is also important for defining adaptation and mitigation actions in response to air pollution trends and air temperature change [11].

The analysis of air temperature is important because of its direct and major effects on the various climatic processes occurring on earth. Indeed, air temperature variability can influence a number of elements, such as relative air humidity [12], evapotranspiration [13], atmospheric pressure and convective movements [14], soil water availability and/or drought [15, 16], and environmental and human discomfort [17].

Overall, rising temperatures can cause a variety of ecological and social problems, particularly in economically vulnerable regions such as the Mediterranean [18]. The southern part of the Mediterranean Basin is most likely to be affected by the effects of rising temperatures, due to its adoption of the agricultural sector as the basis for economic development. The impact of this phenomenon on crop yields, which depend largely on variations in atmospheric temperature, has been observed in other regions of the world. Indeed, agricultural incomes have been reduced by 15–35% in Africa and West Asia and by 25–35% in the Middle East, due to a temperature rise of only 2–4°C [19, 20].

Studies have been carried out in many parts of the world to measure trends/changes in air temperature behavior and/or the respective associated impacts. In its sixth report published in 2021, the IPCC [21] shows that temperatures have risen faster over the last 50 years than over the last two millennia and that a warming of 1.1°C has occurred over the last 150 years, with fossil fuel combustion being the main cause. It has also been pointed out that, on current trends, the planet will warm by 1.5°C in all scenarios, reaching this level in the 2030s [22].

Furthermore, the variability and trends in air temperature were the subject of several scientific publications worldwide. The main common conclusion is that there are significant trends towards an increase in mean annual temperature. This result has been observed in South America [23], Central America [16], Kenya [24], Russia [25], Japan [26], East and West Africa [27, 28], Canada [23], the southwestern USA [29], and Nepal [30]. Schaefer and Domroes (2009) [31] analyzed the mean daily temperature of numerous stations in Japan and observed an upward trend in annual temperature from 0.35°C to 2.93°C over a 100 year period (1991–2000). Caloiero [32] concluded that there is a positive trend in maximum and minimum

temperatures, particularly for the autumn-winter period at the New Zealand level.

In the Mediterranean region, classified as one of the areas likely to be most affected by climate change, several studies have shown a positive and statistically significant trend in mean annual temperature. Examples include the study by Chaouche et al. on the Mediterranean part of France [33], Rio et al. [34] and Hidalgo et al. [35] on Spain, Yılmaz [36] on Turkey, Brunetti et al. [37] on Italy, Kalamaras et al. [38] on Greece, and Boudiaf et al. [39] on Algeria.

However, the observation of rising air temperature trends is not unanimous. Some studies have observed signs of opposite air temperature trends (increases and decreases) and nonuniformity, both in time (between months and/or between seasons) and in space (when comparing the same region). This behavior has been observed in Ireland [11], China [17, 40], the USA [20], Aguascalientes, Mexico [41], and Chhattisgarh, India [42], although positive trends have been more common and widespread.

Previous climate studies identify Morocco as one of the countries most affected by the effects of climate change [43]. Recently, Morocco has experienced one of the most extensive periods of drought in its contemporary history, marked by high temperatures and reduced rainfall [43–46].

Other scientific research indicates that this rise in temperatures will continue in the future, although trends in precipitation remain uncertain. Filahi et al. [47] examined the RCP4.5 and RCP8.5 emission scenarios for two future periods, 2036–2065 and 2066–2095. Their conclusion was that, in most regions of Morocco, the minimum temperature will increase more than the maximum temperature. Recent projections for certain regions of Morocco predict a future reduction in precipitation, with negative implications for water resources and worsening drought [47–49]. In addition, several drought analyses and future temperature projections predict a systematic increase in maximum and minimum temperatures, ranging from 1 to 6°C [50, 51]. Ouhamdouch et al. [52] predict a sharp increase in the estimated mean annual temperature of 0.72°C between 2010 and 2050 in the Essaouira Basin, west-central Morocco. Khomsi et al. [50] suggested that extreme temperature trends are predominantly positive in the country's two major watersheds, Tensift and Bou Regreg. The same result was observed by Hadri et al. [18] in the Chichaoua region.

Although numerous studies have been carried out on climate change in various regions of Morocco, particularly in the center of the country, there is a lack of studies concerning the Moulouya Basin, which encompasses the northeastern part of the country. In this context, the main aim of the present work is to fill this gap by examining trends in mean monthly temperature and its spatial and temporal variability.

2. Materials and Methods

2.1. Study Area Description. The Moulouya watershed, one of Morocco's largest watersheds, encompasses an area of approximately 55,000 square kilometers, as reported by the

Agence du Bassin de la Moulouya (ABHM). This vast region covers much of northeastern Morocco, as illustrated in Figure 1. The primary Moulouya River stretches over a distance of 600 kilometers, originating at the confluence of the Middle and High Atlas Mountains and flowing northeastward to the Mediterranean at Ras El Ma [53]. Administratively, this basin extends across the territories of the provinces of Nador, Figuig, Jerada, Oujda-Angad, Berkane, Taourirt, Guercif, Taza, Boulemane, Midelt, and Khénifra, collectively housing a population exceeding 2.5 million residents.

Moulouya's water supply plays a significant role in the national agricultural economy [54]. According to data from the French Ministry of Agriculture, Maritime Fishing, Rural Development, and Water and Forestry, the eastern administrative region, which comprises the first seven provinces mentioned, contributes approximately 14% to citrus fruit production, 10% to olive production, 9% to sugar beet production, and 8% to red meat production [55].

The expansive and diverse topography of the Moulouya watershed gives rise to a wide range of climatic conditions. These conditions span from a Mediterranean climate in the lower Moulouya to a relatively cooler continental climate in the upper Moulouya and even to an arid, Saharan-like climate in the Guercif Basin and the mountainous regions of the middle Moulouya [56–58]. Annual rainfall levels are relatively low and erratic, with cumulative annual precipitation ranging from less than 100 mm to slightly over 600 mm, depending on the specific region [59]. Snowfall is generally observed at altitudes above 1,500 meters and persists primarily above 2,000 meters, primarily on the peaks of the Middle and High Atlas, with an occasional presence on the high plateaus.

2.2. Observed Climate Data Sources and Station Selection.
The data used in this research relate to monthly average air temperatures measured at 2 m above the surface. These temperature records were obtained, as daily data, from the archives of the Moulouya Hydraulic Basin Agency (ABHM) and the Météorologie Nationale, encompassing data collected by nine recording stations located in and around the Moulouya Basin (as shown in Figure 1 and detailed in Table 1). These datasets were selected based on several criteria, including data quality, reliability, geographical distribution, and the extent of temporal gaps in their records. Consequently, the length of time over which temperature records were taken was a crucial factor in capturing the temporal variability of mean monthly temperatures, and our dataset covers the period from 1980 to 2020.

Unfortunately, the coverage of measuring stations in the catchment is not optimal, with a notable shortage of stations in the eastern part of the catchment. It should also be noted that the majority of these monitoring stations are located at relatively low altitudes, which may impose certain limitations on the applicability of the results generated in our study.

In addition, as is the case in many parts of the world, some of our data series have gaps that need to be filled. Indeed, to obtain optimum results, we have exclusively used series with data gaps of between 2% and 10%. In this context, the stations presenting the longest time series are those of Guercif (S2), Dar Ben Driouech (S8), Ain Bni Mathar (S6), Oujda (S5), and Louggarh (S7) with a percentage of missing data of 2.5%, 3.4%, 2.7%, 5.4%, and 4%, respectively.

Furthermore, the stations of Melg El Ouidane (S9), Belpahar (S1), Bab Marzouka (S4), and Outat El Haj (S3) present percentages of missing data estimated at 6.7%, 7.4%, 8.7%, and 8.9%, respectively. These values are already considered acceptable for the application of some of the most widely recognized quality methods and tests, enabling gaps to be filled effectively. To this end, in order to test data quality, we opted for the Climatol tool (version 3.1.1, https://www.climatol.eu/, downloaded on December 15, 2022). This tool is recommended by several climatologists [56, 60–62]. The stations where data were collected are summarized in the table as follows.

The mean annual temperature in the Moulouya watershed varies between 18 and 20°C at six stations: S1, S2, S3, S4, S8, and S9. These stations are mainly located in the center or downstream of the watershed, at altitudes below 1000 meters. Upstream, however, temperatures are lower, reaching 11.2°C at station S7, which is located at an altitude of over 2,500 meters.

The average monthly temperature can reach 30°C during July at station S2, but does not exceed 19.7°C at station S7 for the same month. The coldest month in the Moulouya Basin is January, with average temperatures ranging from 11.5°C at Melg El Ouidane Station (S9) to 3.4°C at Louggarh Station (S7).

2.3. Methodology Adopted.
A review of the scientific literature reveals that the majority of climate researchers have used recommended statistical tests to analyze variability, trends, and breakpoints within time series [63–67]. In this context, to accurately identify the variability, trends, and change points in mean monthly temperature in the Moulouya watershed, we have selected the following statistical tests.

2.3.1. Mann–Kendall Trend Test.
As we mentioned in the introduction, to analyze trends in monthly data series, the classic Mann–Kendall test [68, 69] is used. Statistical trend tests identify and/or estimate the existence or not of a trend in a time series according to the desired degree of significance. Mann–Kendall is a nonparametric test requiring only that the data be serially independent, without assuming the normality of the distribution [70, 71]. The Mann–Kendall statistic S is calculated as follows:

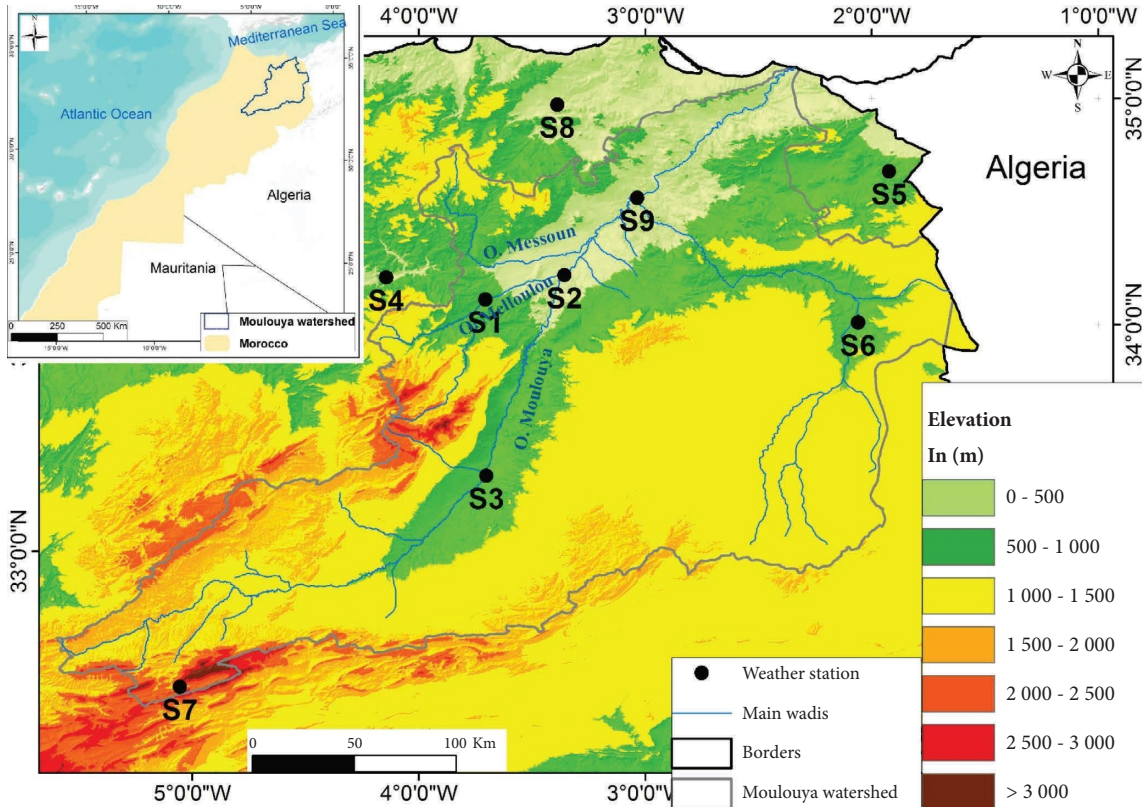$$S = \sum_{i=1}^{n-1} \sum_{j=i+1}^{n} \text{sgn}(x_j - x_i), \tag{1}$$

FIGURE 1: Geographical location of the Moulouya watershed.

TABLE 1: Geographical locations of stations.

Name	ID	Longitude	Latitude	Elevation
Belpahar	S1	−3.70505	34.11262	512
Guercif	S2	−3.35731	34.21953	362
Outat El Haj	S3	−3.70184	33.33271	763
Bab Marzouka	S4	−4.1453	34.20946	398
Oujda	S5	−1.92333	34.67846	450
Bni Mathar	S6	−2.06034	34.01057	921
Louggarh	S7	−5.05607	32.40132	1925
Dar Driouch	S8	34.97262	−3.38898	289
Melg El Ouidane	S9	−3.0358	34.56117	268

Code of the coordinate system used is EPSG: 26191.

where n is the length of the data series and x_i and x_j are the data value in time series i and j $(j > i)$, respectively, with sgn $(x_j - x_i)$ responding to the following sign function:

$$\text{sgn}\left(x_j - x_i\right) = \begin{cases} 1, & \text{if } x_j - x_i > 0, \\ 0, & \text{if } x_{j-x_i=0} - 1, \text{if } x_j - x_i < 0. \end{cases} \quad (2)$$

The variance (V) of S is calculated as follows:

$$V(s) = \frac{n(n-1)(2n+5) - \sum_{k=1}^{m} t_k(t_k - 1)(2t_k + 5)}{18}. \quad (3)$$

In the above equation, n is the number of data points, m is the number of linked groups, and t_k is the number of links of extent k. A related group is a set of data samples with the same value. In cases where the sample size n is greater than

10, the standard normal test statistic ZS is calculated using the following equation:

$$Z = \begin{cases} \dfrac{S-1}{\sqrt{\text{var}(s)}}, & \text{if } S > 0, \\ 0, & \text{if } S = 0, \\ \dfrac{S+1}{\sqrt{\text{var}(s)}}, & \text{if } S < 0. \end{cases} \quad (4)$$

Positive Z values indicate increasing trends, while negative values indicate decreasing trends. The trend test is performed at a specific α significance level. When $|Z| > Z_1 - \alpha/2$, the null hypothesis is rejected and a significant

trend exists in the time series. $Z_1 - \alpha/2$ is obtained from the standard normal distribution table [72]. In this study, the significance levels chosen are as follows: $\alpha = 0.01$ (or 99% confidence interval), $\alpha = 0.05$ (or 95% confidence interval), and $\alpha = 0.1$ (or 90% confidence interval). At the level of significance of 1%, 5%, and 10%, the null hypothesis "absence of trend" is rejected if $|Z| > 2.57$, $1.96 \le |Z| < 2.57$, and $1.64 \le |Z| < 1.96$ [73], respectively. Kisi and Ay [74] stated that in the case of long-term rainfall trend analysis, the MK test performs better than parametric tests.

The magnitude of a trend in a time series, such as the amount of change per year, can be estimated using a nonparametric method known as Sen's estimator [75]. A positive value of Sen's slope indicates an upward trend, and a negative value indicates a downward trend in the time series.

2.3.2. Mann–Kendall Sequential Test (SQMK).

Using the traditional Mann–Kendall test to detect the general trend of a statistical series over an extended period does not provide an exhaustive picture of the trend structure across the whole series. These fluctuations can be detected by applying the sequential test for each individual subperiod [76]. Makokha and Shisanya [77] have shown that negative or positive trends are not always significant for the entire time series, but can be detected using sequential Mann–Kendall plots. This test was proposed by Sneyers [78] to determine the approximate year of the start of a significant trend. The SQMK test is calculated using the ranked values, y_i of the original values in the analysis $(x_1, x_2, x_3, \ldots, x_n)$. The amplitudes of y_i $(i = 1, 2, 3, ..., n)$ are compared with y_j $(j = 1, 2, 3, ..., i - 1)$. For each comparison, the cases where $y_i > y_j$ are counted and denoted by n_i. The SQMK test establishes two series, a progressive series of $u(t_i)$ and a retrospective series of $u'(t_i)$. The test statistic t is then given by the following equation:

$$t_i = \sum_{j-1}^{i} n_i. \tag{5}$$

The distribution of the test statistic ti has a mean given as follows:

$$E(t_i) = \frac{i(i = 1)}{4}. \tag{6}$$

The variance is calculated as follows:

$$\text{Var}(t_i) = \frac{i(i-1)(2i+5)}{72}. \tag{7}$$

The sequential values of the $u(t_i)$ statistic are then calculated as in following equation:

$$u(t_i) = \frac{t_i - E(t_i)}{\sqrt{\text{Var}(t_i)}}. \tag{8}$$

The retrospective sequential statistic $u'(t_i)$ is estimated in the same way, but starting from the end of the series. The estimated year (time) of onset of the trend is identified by locating the intersection of the progressive $u(t_i)$ and retrograde $u'(t_i)$ curves. The critical value for a 95% confidence level is ±1.96.

2.3.3. Innovative Trend Analysis.

The innovative trend analysis (ITA) method, as introduced by Şen in 2012 [79], has been employed to identify trends in weather series. The ITA method is one of several approaches devised to uncover deterministic trends within observed time series [80].

In the ITA method, the time series is partitioned into two equal segments from the initial date to the end. These two subseries are then sorted in ascending order. The first half of the series is plotted along the X-axis, while the second half is plotted along the Y-axis on a Cartesian coordinate system. When data points align along a 1 : 1 line, it indicates the absence of a discernible trend. If the data points appear above the 1 : 1 line, it suggests a positive trend, while points accumulating below the 1 : 1 line indicate a negative trend [81].

For the ITA, we utilized the "trendchange" package within R software version 4.0.2 (R Core Team 2020). In this study, we tested the null hypothesis of no trend against the alternative hypothesis of the presence of a trend in the precipitation time series at two different significance levels (α): $\alpha = 5\%$ and $\alpha = 1\%$.

2.3.4. Pettitt's Test.

This is a powerful method for highlighting the stationary or nonstationary nature of time series. The test examines the existence of a break at an unknown time (t) in the series, using a formula derived from Mann–Whitney. According to the Pettitt test, $x_1, x_2, x_3, \ldots x_n$ is an observed data series that has a change point at t such that $x_1, x_2, \ldots, x_t$ has a distribution function $F_1(x)$ that is different from the distribution function $F_2(x)$ of the second part of the series $x_{t+1}, x_{t+2}, x_{t+3} \ldots, x_n$ [82]. The U_t nonparametric test statistic for this test can be described as follows:

$$U_t = \sum_{i=1}^{t} \sum_{j=t+1}^{n} \text{sign}(x_t - x_j),$$

$$\text{sign}(x_i - x_j) = \begin{bmatrix} 1, & if(x_i - x_j) > 0, \\ 0, & if(x_i - x_j) = 0, \\ -1, & if(x_i - x_j)0. \end{bmatrix}. \tag{9}$$

The test statistic K and the associated confidence level (ρ) for the sample length (n) can be described as follows:

$$K = \max |U_t|,$$

$$\rho = \exp\left(\frac{-K}{n^2 + n^3}\right). \tag{10}$$

When ρ is below the specific confidence level, the null hypothesis is rejected. The approximate probability of significance (p) for a point of change is defined as follows:

$$p = 1 - \rho. \tag{11}$$

Clearly, when there is a significant change point, the series is segmented at the change point into two subseries. The K test statistic can also be compared with standard values at different confidence levels for the detection of a change point in a series.

2.3.5. Buishand's Range Test. This approach was proposed by Buishand in 1982 [83]. It applies to normal distributions and assumes no change in the variance of the distribution. Assume an a priori uniform distribution for the position of the change point. The adjusted partial sum (S_k), i.e., the cumulative deviation from the mean for the kth observation of a series $x_1, x_2, x_3, \ldots, x_k, \ldots, x_n$ with mean $\overline{x}$, can be calculated using the following equation:

$$S_k = \sum_{i=1}^{k} (x_i - \overline{x}). \tag{12}$$

A series can be homogeneous, with no change point, if $S_k \cong 0$, because in a random series, the deviation from the mean will be distributed on either side of the series mean. The significance of the change can be assessed by calculating the adjusted revaluation range (R) using the following equation:

$$R = \frac{\text{Max}\,(S_k) - \text{Min}\,(S_k)}{\overline{x}}. \tag{13}$$

2.3.6. von Neumann Ratio Test. The von Neumann ratio test [84] is also one of the statistical tests used to detect points of change within time series. The statistics of this test in a series of observations $x_1, x_2, x_3, \ldots, x_n$ can be described as follows:

$$N = \frac{\sum_{i=1}^{n-1} (x_i - x_{i-1})^2}{\sum_{i=1}^{n} (x_i - \overline{x})^2}. \tag{14}$$

According to this test, if the sample or series is homogeneous, then the expected value $E(N) = 2$ under the null hypothesis of constant mean. If the sample shows a point of change, then the value of N must be less than 2, otherwise we can assume that the sample shows a rapid variation in the mean.

The P value was used to determine the degree of significance of each point of change in the time series.

3. Results

The results of the Mann–Kendall test show that, in the Moulouya watershed, the average monthly temperature between 1980 and 2020 is increasing across the board. Z values exceed the 5% significance level for April, May, June, July, August, and October (Table 2). According to the Sen slope test, mean monthly temperatures show an annual increase of between 0 and 0.13°C. The maximum value is recorded in July, specifically at station S5. On an overall watershed scale, May, August, and July show a rapid

warming trend, with average rates of 0.093, 0.086, and 0.8°C per year, respectively. By contrast, the series for the other months shows no significant trend (Table 3).

The Mann–Kendall sequential test is a method essentially designed to determine the start dates of each trend and identify any shorter trends present. According to the results of the analysis (Figure 2), the most significant trends during January were observed at stations S1, S3, S4, and S8. These trends were initiated in 1995 at all four stations and continued until 2015, 2018, 2009, and 2020, respectively (Figure 2).

However, no significant trend was observed in the February data series for the entire study area. For March, only station S7 showed a significant upward trend between 2010 and 2020. For April, almost all stations showed a significant trend between 2014 and 2020. Similarly, May follows a comparable trend, with significant trends appearing at certain stations from 1995 onward. During the summer months, particularly significant and widespread trends were observed at all stations, with the exception of station S7, located in the watershed uplands at an altitude of 1925 meters. These trends began between 2000 and 2010 and continued until the end of the study period. A similar pattern emerges in October, although the degree of significance is relatively lower than in the summer months. For September, November, and December, no significant trend was detected. The $U(t)$ curves oscillated between the two test thresholds, i.e., ±1.96 times the standard error.

The ITA method was only applied to mean annual temperatures. The results show that most data points lie above the 1:1 line, indicating an overall upward trend between the first and second halves of the time series. However, the patterns observed at individual stations show distinct characteristics (Figure 3). This result confirms that of the classic Mann–Kendall test.

In this study, the Mann–Kendall sequential test was used to extract partial trends from the data series, while the Pettitt, Buishand, and von Neumann tests were applied to detect points of change. The results of the Pettitt test revealed significant change points in 5 stations for the data series for January, a single point for February, and 2 significant points for March. From April to October, the data series appear to be heterogeneous, with the widespread emergence of change points. The dates of these points are not similar at all stations and for all months (Tables 4 and 5). However, it is notable that most of these points of change occurred around 2000 and 2010.

The results obtained from the Buishand test reflect similar conclusions to those of the Pettitt test. They also indicate that most of the significant change points are located in the data series corresponding to the spring and summer seasons, extending from April to August. The dates of these change points show similarities with those detected by the Pettitt test (Tables 4 and 5).

The von Neumann test has also proven its effectiveness in identifying change points. Its results show that the majority of change points are detected during the summer season. On the one hand, the data series corresponding to January and December are also heterogeneous and present

Table 2: Results of the Mann–Kendall test applied to monthly mean temperature data between 1980 and 2020 in the Moulouya watershed.

Time series	January	February	March	April	May	June	July	August	September	October	November	December
S1	1.21	−0.30	0.33	2.63***	3.70***	3.37***	3.96***	4.53***	1.51	2.78***	−0.17	−0.49
S2	1.37	0.27	−0.24	2.60***	2.80***	3.42***	3.73***	3.29***	1.95*	2.55**	0.18	0.06
S3	1.42	0.28	0.94	1.71*	3.69***	2.84***	3.32***	3.32***	1.26	2.16**	0.72	0.21
S4	0.61	−1.14	−0.24	2.26**	3.99***	3.00***	3.75***	4.04***	1.72*	1.85*	−0.01	−0.83
S5	−0.43	−0.35	1.18	3.19***	4.88***	4.95***	5.23***	4.36***	1.98**	2.13**	−1.57	−1.87*
S6	0.92	0.08	0.96	2.92***	3.53***	2.93***	3.18***	4.21***	1.02	3.24***	1.12	1.14
S7	1.71	1.39	2.07**	2.80***	2.25**	0.00	0.80	−0.67	−2.15**	2.15**	1.16	1.16
S8	2.54**	0.90	0.93	2.94***	4.00***	2.92***	3.60***	3.46***	1.62	3.30***	0.65	−0.26
S9	0.89	−0.62	0.52	3.14***	3.56***	3.81***	4.23***	4.69***	1.72	1.57	−0.61	−0.38

*Trends at the 0.1 significance level if 1.64_Z < 1.96. **Trends at the 0.05 significance level if 1.96_Z < 2.57. ***Trends at the 0.01 significance level if 2.57 < Z.

Table 3: Results of Sen's slope estimator (in degrees per year) applied to monthly mean temperature data between 1980 and 2020 in the Moulouya watershed.

Time series	January	February	March	April	May	June	July	August	September	October	November	December
S1	0.033	−0.004	0.006	0.045	0.090	0.083	0.093	0.095	0.029	0.047	−0.001	−0.009
S2	0.031	0.005	−0.001	0.046	0.080	0.075	0.082	0.086	0.029	0.055	0.004	0.000
S3	0.039	0.008	0.016	0.048	0.103	0.067	0.086	0.085	0.028	0.050	0.018	0.004
S4	0.012	−0.023	−0.004	0.050	0.104	0.083	0.100	0.104	0.044	0.043	0.000	−0.017
S5	−0.007	−0.007	0.014	0.064	0.126	0.116	0.133	0.101	0.036	0.040	−0.038	−0.046
S6	0.020	0.000	0.021	0.063	0.106	0.072	0.083	0.100	0.021	0.080	0.026	0.028
S7	0.045	0.028	0.038	0.055	0.053	0.000	0.012	−0.009	−0.027	0.038	0.017	0.032
S8	0.046	0.017	0.016	0.042	0.070	0.060	0.065	0.064	0.020	0.060	0.010	−0.005
S9	0.027	−0.014	0.010	0.061	0.105	0.086	0.118	0.096	0.036	0.042	−0.015	−0.010

statistically significant change points (Tables 4 and 5). On the other hand, the data series for the other months are relatively homogeneous and show no statistically significant points of change.

On an annual scale, all mean annual temperature series recorded at the 9 stations in the Moulouya watershed are statistically heterogeneous. The points of change are significant at the 1% threshold. Their dates vary from station to station, depending on geographical location, recording conditions, and data reliability (Table 6).

4. Discussion

The aim of our study is to highlight the spatiotemporal variability of mean monthly temperature in the Moulouya watershed, while analyzing the resulting trends. We used monthly mean temperature data from nine measuring stations belonging to the Moulouya Watershed Agency (ABHM), carefully selected based on their reliability, the length of their records, and their geographical location within the basin. Despite efforts to homogenize and improve data quality, the spatial coverage of measuring stations in the study area is relatively poor, and their geographical distribution is unbalanced, with a greater concentration in the downstream part of the basin than in the upstream part. This observation raises the possibility that the reality of spatial temperature variability throughout the basin may be significantly obscured. However, adding temperature data from other major watersheds in Morocco could help clarify differences in warming rates across elevations.

The results reveal significant upward trends across the board, particularly observed in the summer months. The results reveal significant upward trends across the board, particularly observed in the summer months. Application of the Mann–Kendall sequential test to the monthly mean temperature series indicates that this upward trend began in 2000. On average, this increase is estimated at 0.093°C/year across the entire Moulouya watershed. These consistent results are in line with the conclusions of the IPCC report published in 2021, which demonstrated an increase in average air temperature of around 0.85°C between 1880 and 2012. The same report addressed the fact that between 2011 and 2020, the average temperature of the earth's surface was 1.1°C higher than the average temperature at the end of the nineteenth century (before the rapid increase in greenhouse gas concentrations). It was also the highest in the last 100,000 years [21]. The last three decades are considered the warmest since 1850. These data clearly show that the rise in temperatures over the last 50 years has been faster than over the last two millennia, with a warming of 1.1°C over the last 150 years.

While the IPCC reports have been produced in summary form, several researchers have carried out studies of air temperature variability and trends in specific terrains. The main conclusions concur in showing significant trends towards an increase in mean annual temperature. In this context, Eybekoğlu and Aktürk found that summer temperatures increased in a watershed located in the central part of Turkey. These trends were statistically significant at the 95% confidence level at all stations [85]. Swain et al. observed
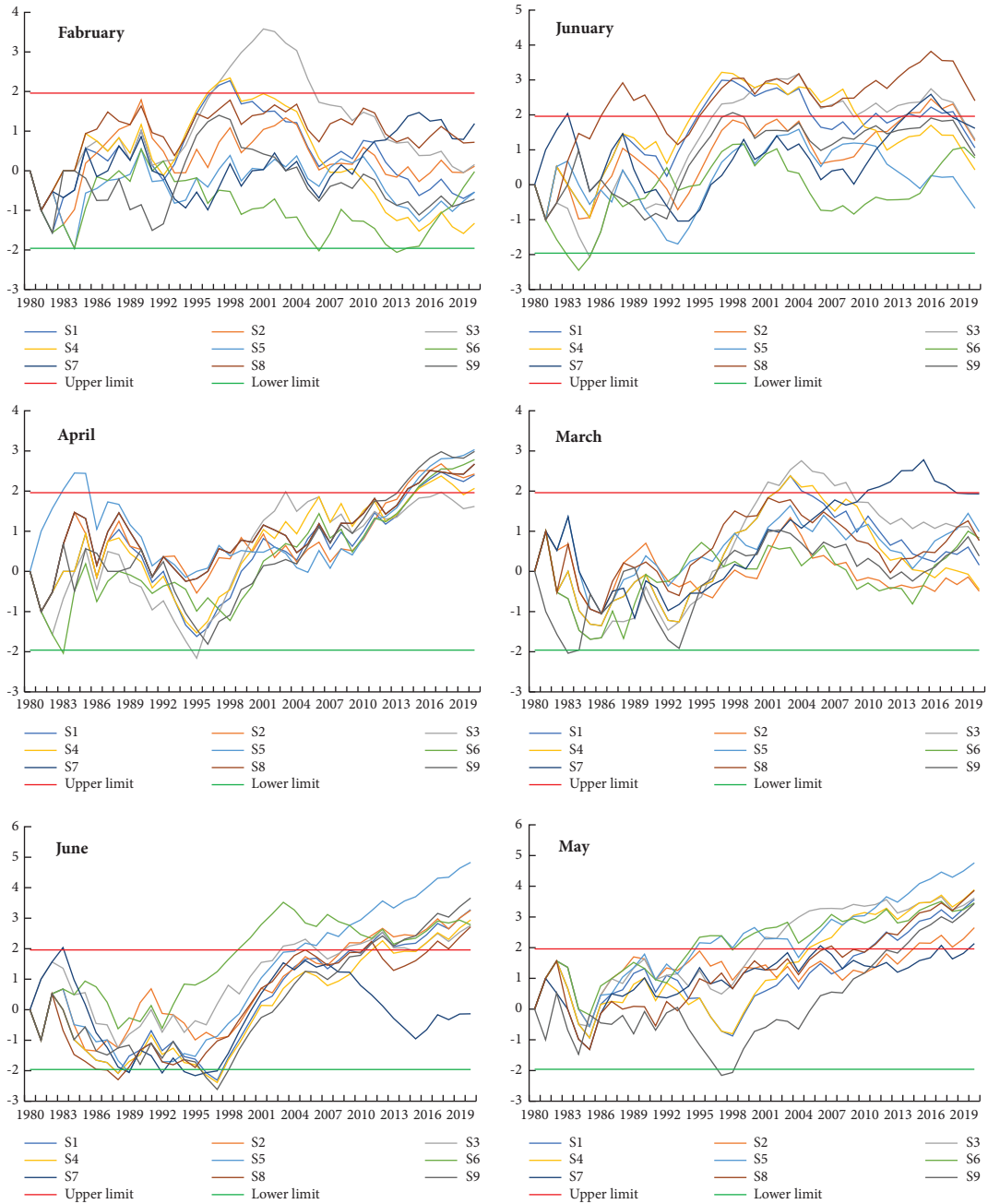
(a)

Figure 2: Continued.

(b)
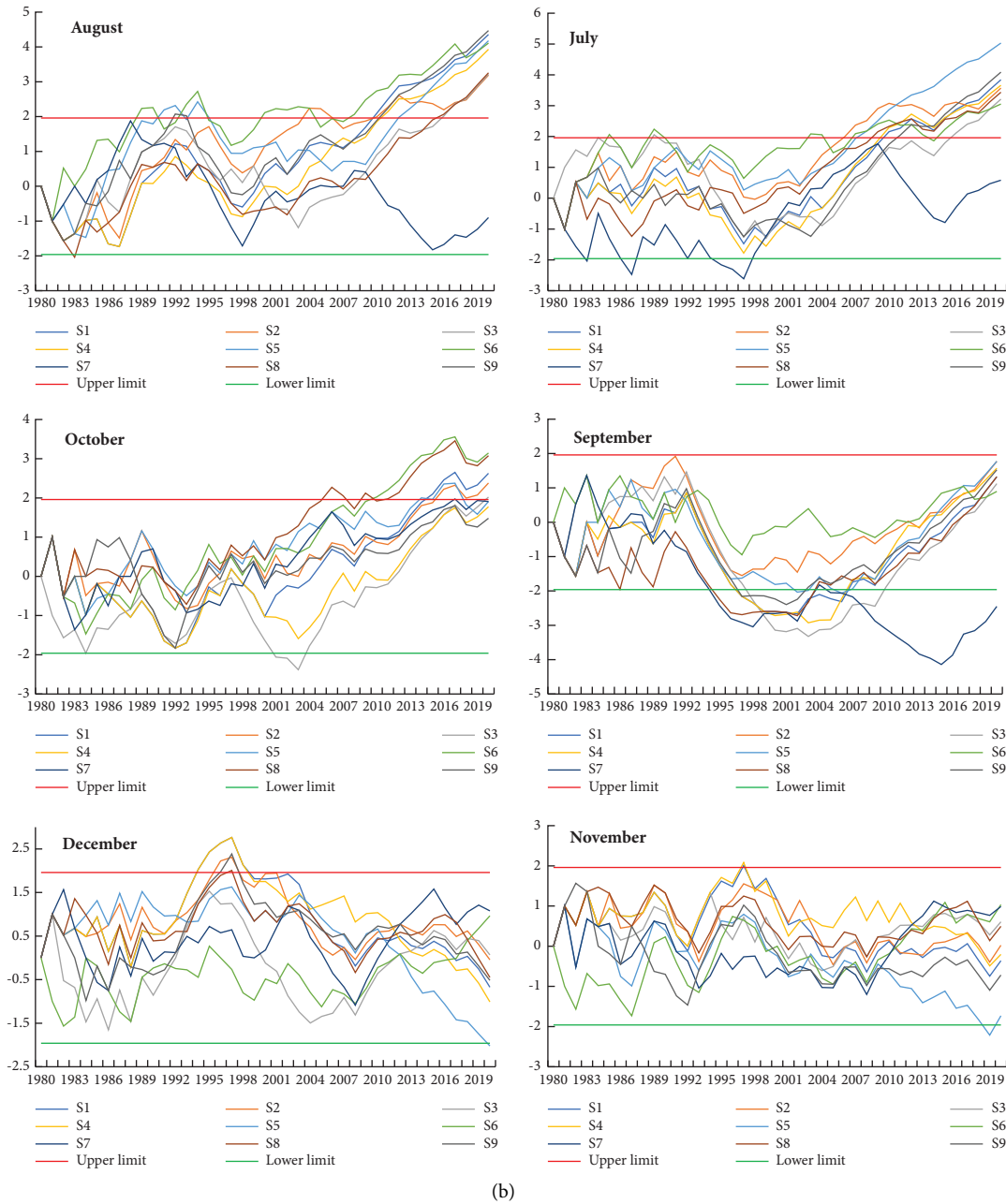
FIGURE 2: Results of the Mann–Kendall sequential test applied to monthly mean temperature data between 1980 and 2020 in the Moulouya watershed. (a) Between January and June and (b) between July and December.

that the mean annual temperature increased by 1.44% between 1901 and 2002 in the Chhattisgarh area of western India [86]. Moreover, the increase in mean annual temperature appears to be global in character. In fact, rising trends have been observed in America [16, 23, 29], Canada [28], Africa [24, 27], Russia [25], and Japan [26].

In the same context, in the Mediterranean region, the majority of studies carried out on the analysis of temperature trends have shown a significant trend towards an increase in mean annual temperature [33–39]. It should be noted that, on a seasonal scale, most of these studies have focused on an increase in summer or autumn temperatures.
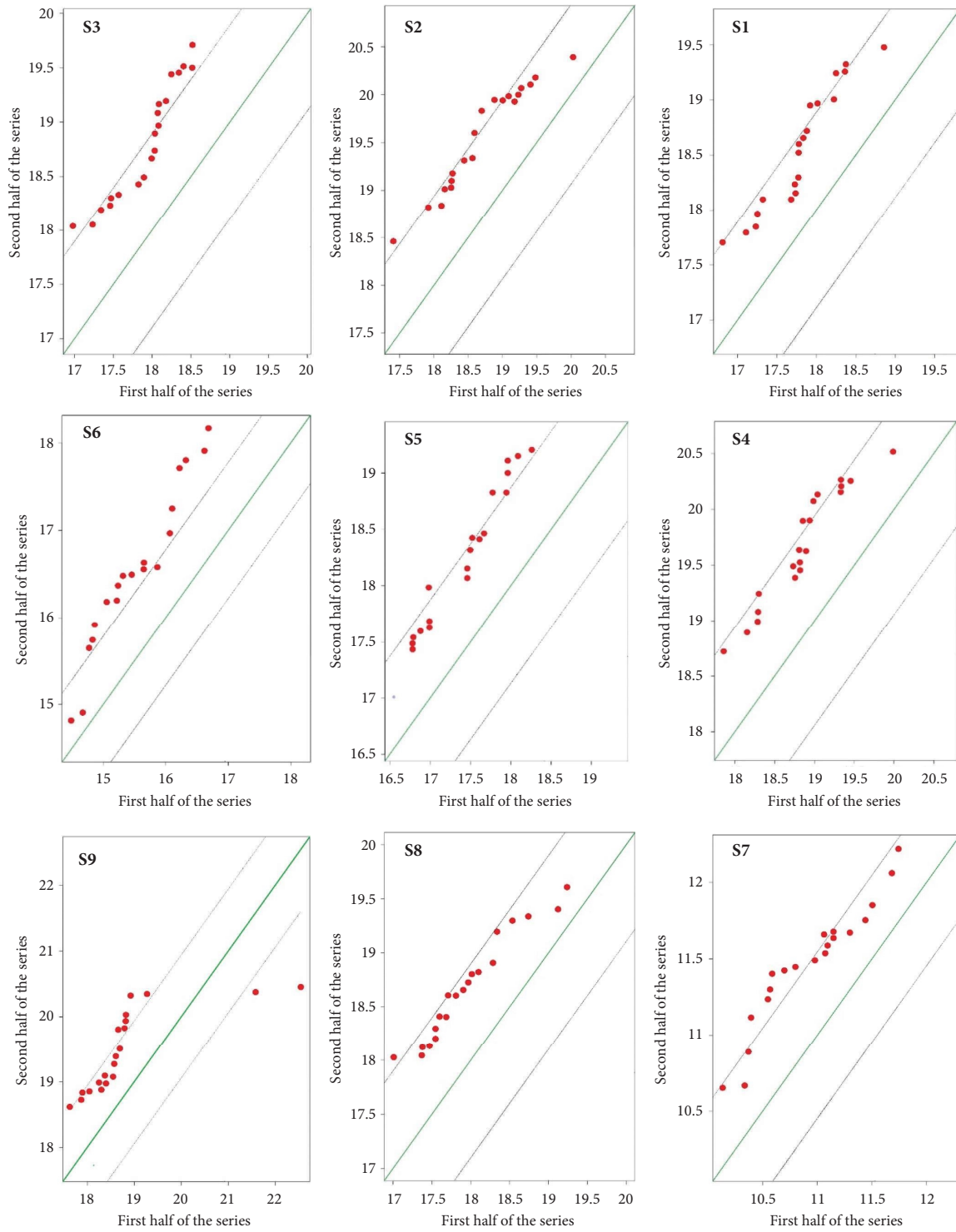
FIGURE 3: Results of the ITA method applied to mean annual temperature data between 1980 and 2020 in the Moulouya watershed.

TABLE 4: Results of the 3 change point detection methods applied to monthly mean temperature data, January–June, between 1980 and 2020 in the Moulouya watershed.

	January			February			March			April			May			June		
	P value	Significance	Date	P value	Significance	Date	P value	Significance	Date	P value	Significance	Date	P value	Significance	Date	P value	Significance	Date
Pettitt's test																		
S1	0.023	*	1992	0.625	N	—	0.161	N	—	≤0.01	**	1996	≤0.01	***	1998	≤0.001	***	1997
S2	0.156	N	—	0.878	N	—	0.646	N	—	0.013	*	2007	0.068	N	—	≤0.001	***	1998
S3	≤0.01	***	1992	0.207	N	—	0.031	*	1995	≤0.001	***	1995	≤0.001	***	1998	≤0.01	***	1996
S4	0.048	*	1992	0.036	*	2004	0.305	N	—	0.021	*	1996	≤0.001	***	1998	≤0.001	***	1997
S5	0.468	N	—	0.798	N	—	0.550	N	—	≤0.01	***	2007	≤0.001	***	2004	≤0.001	***	1999
S6	0.448	N	—	0.303	N	—	0.287	N	—	≤0.01	***	2009	≤0.01	***	1993	≤0.01	***	1992
S7	0.087	N	—	0.109	N	2006	0.021	*	1999	≤0.01	**	1997	0.161	N	—	0.378	N	—
S8	0.010	**	1994	0.390	N	1993	0.176	N	—	0.014	*	2004	≤0.01	***	2004	≤0.01	***	1998
S9	0.013	*	1992	0.089	N	1998	0.234	N	—	≤0.01	***	1996	≤0.001	***	1998	≤0.001	***	1997
Buishand's range test																		
S1	0.114	N	—	0.439	N	—	0.130	N	—	0.013	*	1996	≤0.001	***	1998	≤0.001	***	1997
S2	0.305	N	—	0.876	N	—	0.725	N	—	≤0.01	**	2007	0.030	*	2004	≤0.001	***	1999
S3	0.015	*	1992	0.175	N	—	0.020	*	1995	≤0.001	***	1995	≤0.001	***	1998	≤0.01	***	1996
S4	0.220	N	—	0.020	*	2004	0.279	N	—	0.065	N	—	≤0.001	***	1998	≤0.001	***	1997
S5	0.268	N	—	0.682	N	—	0.448	N	—	≤0.001	***	2007	≤0.001	***	2004	≤0.001	***	1999
S6	0.364	N	—	0.318	N	—	0.349	N	—	≤0.01	***	2009	0.015	*	1994	≤0.01	***	1992
S7	0.044	*	2009	0.183	N	—	0.028	*	1999	≤0.01	***	1997	0.167	N	—	0.192	N	—
S8	0.147	N	—	0.396	N	—	0.200	N	—	0.01	**	2004	≤0.01	***	2004	0.011	*	1998
S9	0.142	N	—	0.012	*	1998	0.218	N	—	≤0.01	***	1996	≤0.001	***	1998	≤0.001	***	1997
von Neumann ratio test																		
S1	≤0.001	***		0.020	*		0.139	N		0.26	N		0.026	*		≤0.01	**	
S2	≤0.01	***		0.566	N		0.135	N		0.256	N		0.271	N		0.075	N	
S3	≤0.001	***		≤0.01	***		≤0.01	***		≤0.01	**		≤0.001	***		0.195	N	
S4	≤0.001	***		≤0.01	***		≤0.01	***		0.278	N		≤0.01	***		≤0.01	***	
S5	≤0.01	***		0.738	N		0.223	N		≤0.01	***		≤0.01	***		≤0.001	***	
S6	≤0.01	**		0.098	N		0.450	N		0.026	*		0.074	N		0.131	N	
S7	≤0.01	**		0.518	N		0.607	N		0.03	*		0.604	N		0.015	*	
S8	≤0.001	***		0.494	N		0.151	N		0.07	N		≤0.01	***		≤0.01	***	
S9	≤0.001	***		≤0.001	***		0.164	N		0.02	*		≤0.001	***		0.011	*	

N, no significant change point. *Significant point of change at 0.1 level. **Significant point of change at 0.05 level. ***Significant point of change at 0.01 level. *Significant change point at 0.1 threshold. **Significant change point at 0.05 level. ***Significant change point at 0.01 threshold.

TABLE 5: Results of the 3 change point detection methods applied to monthly mean temperature data, July–December, between 1980 and 2020 in the Moulouya watershed.

	July			August			September			October			November			December		
	P value	Significance	Date	Significance	Date	P value	Significance	Date	P value	Significance	Date	P value	Significance	Date	P value	Significance	P value	Date
Pettitt's test																		
S1	≤0.001	***	2004	***	2002	0.023	*	2009	≤0.01	**	2000	0.712	N	—		N	0.483	—
S2	≤0.001	***	2002	***	1999	0.069	—	—	0.028	*	2003	0.946	N	—		N	0.866	—
S3	≤0.001	***	2004	***	2003	0.010	*	2009	≤0.01	***	2003	0.549	N	—		N	0.448	—
S4	≤0.001	***	2002	***	2003	≤0.01	***	2005	0.015	*	2004	0.858	N	—		N	0.299	—
S5	≤0.001	***	2005	***	2009	≤0.01	***	2009	0.145	N	—	0.217	N	—		*	0.021	2010
S6	≤0.01	**	1997	***	1998	0.495	—	—	≤0.01	***	2000	0.185	N	—		*	0.044	2008
S7	0.091	N	—	N	—	≤0.01	**	1992	0.023	*	2000	0.056	*	###		N	0.246	—
S8	≤0.001	***	2002	***	2002	0.040	*	2009	≤0.01	***	2000	0.793	N	—		N	0.561	—
S9	≤0.001	***	2003	***	2002	0.023	*	2009	0.101	N	—	0.464	N	—		N	0.708	—
Buishand's range test																		
S1	≤0.001	***	2004	***	2002	0.037	*	2006	≤0.01	**	2000	0.51	N	—		N	0.137	—
S2	≤0.01	***	2002	***	1998	0.079	N	—	0.019	*	2003	0.9	N	—		N	0.702	—
S3	≤0.001	***	2004	***	2003	0.049	*	2003	0.010	**	2003	0.83	N	—		N	0.711	—
S4	≤0.001	***	2005	***	2003	≤0.01	***	2005	0.019	*	2004	0.9	N	—		N	0.136	—
S5	≤0.001	***	2005	***	2009	0.020	*	2009	0.097	N	—	0.25	N	—		*	0.043	2010
S6	≤0.01	***	1997	***	1998	0.897	N	—	≤0.01	***	2000	0.22	N	—		*	0.041	2008
S7	0.588	N	—	N	—	0.032	*	1992	0.029	*	2000	0.04	*	###		N	0.619	—
S8	≤0.01	***	2002	***	2009	0.040	*	2009	≤0.01	***	2000	0.91	N	—		N	0.527	—
S9	≤0.001	***	2003	***	1998	0.087	N	—	0.106	N	—	0.12	N	—		N	0.054	—
von Neumann ratio test																		
S1	≤0.001	***		***		≤0.001	***		≤0.001	N		0.136	N		0.507	***	≤0.01	
S2	≤0.001	***		***		≤0.01	***		≤0.01	N		0.399	N		0.760	N	0.456	
S3	≤0.01	***		***		≤0.001	***		≤0.001	***		≤0.01	N		0.989	N	0.051	
S4	≤0.001	***		***		≤0.001	***		≤0.001	N		0.225	N		0.978	***	≤0.01	
S5	≤0.001	***		***		≤0.001	***		≤0.01	N		0.647	N		0.480	N	0.435	
S6	0.012	*		*		≤0.01	N		0.634	N		0.119	N		0.199	*	0.038	
S7	≤0.01	***		***		0.011	***		≤0.01	N		0.739	N		0.658	N	0.243	
S8	≤0.01	***		***		≤0.001	***		≤0.001	N		0.466	N		0.291	*	0.043	
S9	0.011	*		*		0.042	***		≤0.001	N		0.645	*		0.025	***	≤0.001	

N, no significant change point. *Significant point of change at 0.1 level. **Significant point of change at 0.05 level. ***Significant change point at 0.01 threshold.

TABLE 6: Results of the 3 change point detection methods applied to mean annual temperature data between 1980 and 2020 in the Moulouya watershed.

	Pettitt's test			Buishand's range test			von Neumann ratio test		
	P value	Significance	Date	P value	Significance	Date	P value	Significance	Date
S1	≤0.01	***	1999	≤0.001	***	2008	≤0.001	***	
S2	≤0.001	***	1999	≤0.001	***	1999	≤0.001	***	
S3	≤0.001	***	2000	≤0.001	***	2003	≤0.01	***	
S4	≤0.001	***	2000	≤0.001	***	2002	≤0.001	***	
S5	≤0.01	***	2005	≤0.001	***	2005	≤0.01	***	
S6	≤0.01	***	2005	≤0.001	***	2005	≤0.001	***	
S7	≤0.001	***	1998	≤0.001	***	1998	0.015	*	
S8	≤0.001	***	1993	≤0.001	***	1993	≤0.001	***	
S9	≤0.001	***	2003	0.013	*	1992	0.290	N	

N, no significant change point, *significant point of change at 0.1 level, **significant point of change at 0.05 level, ***significant change point at 0.01 threshold.

5. Conclusion

The aim of this study was to examine spatiotemporal variability and trends in mean monthly temperature at the scale of the Moulouya watershed, an area renowned for its vulnerability to the effects of climate change. To this end, statistical methods widely recommended by climate researchers were adopted. The results obtained show a significant upward trend in mean monthly temperature, mainly pronounced during the summer months, in the Moulouya watershed. Application of the Mann–Kendall sequential test to the temperature series revealed that this increase began in 2000. Significant trend change points were also identified at the watershed scale, mainly around 2000, with a marked influence on the summer months.

These results demonstrate the relevance and power of the methods used to analyze spatiotemporal temperature variability in this region, as well as to detect the possible impacts of global warming on water resources in a vulnerable area such as the Moulouya Basin. It is important to stress that this study area is characterized by an expansion of irrigated agricultural land, which reinforces the importance of the conclusions obtained for the sustainable management of water resources in this region. In this context, the future of agriculture and the region's water situation remain uncertain. Moreover, adaptation to the challenges of global warming is a crucial issue in Morocco's arid environments, particularly in the Moulouya Basin, which encompasses large tracts of agricultural land.

Data Availability

The data presented in this study are available from the corresponding author upon reasonable request.

Conflicts of Interest

The authors declare that they have no conflicts of interest.

Authors' Contributions

R.A. conceptualized the study, designed the methodology, and involved in formal analysis. R.A. and R.K. provided software. R.A. and N.Y.K. validated the data and wrote the original manuscript and prepared the draft. R.A. and R.K investigated the data. R.A and I.A. curated the data. R.A., N.Y.K., and M.H. wrote, reviewed, and edited the manuscript. R.A. and B.E. visualized the data. N.Y.K., K.O., and M.H. supervised the data. All authors have read and agreed to the published version of the manuscript.

References

[1] Ipcc, "Summary for policymakers," in *Climate Change 2023: Synthesis Report. Contribution of Working Groups I, II and III to the Sixth Assessment Report of the Intergovernmental Panel on Climate Change*, H. Lee and J. Romero, Eds., IPCC, Geneva, Switzerland, 2023.

[2] M. Mudelsee, "Trend analysis of climate time series: a review of methods," *Earth-Science Reviews*, vol. 190, pp. 310–322, 2019.

[3] J. Hansen, R. Ruedy, M. Sato, and K. Lo, "Global surface temperature change," *Review of Geophysics*, vol. 48, no. 4, pp. RG4004–29, 2010.

[4] P. Romilly, "Time series modelling of global mean temperature for managerial decision-making," *Journal of Environmental Management*, vol. 76, no. 1, pp. 61–70, 2005.

[5] L. Ye, G. Yang, E. Van Ranst, and H. Tang, "Time-series modeling and prediction of global monthly absolute temperature for environmental decision making," *Advances in Atmospheric Sciences*, vol. 30, no. 2, pp. 382–396, 2013.

[6] S. Yue and M. Hashino, "Long term trends of annual and monthly precipitation in Japan," *JAWRA Journal of the American Water Resources Association*, vol. 39, no. 3, pp. 587–596, 2003.

[7] Z. Alemu and M. O. Dioha, "Climate change and trend analysis of temperature: the case of Addis Ababa, Ethiopia," *Environ. Syst. Res*, vol. 9, no. 1, 2020.

[8] E. Fischer, U. Beyerle, and R. Knutti, "Robust spatially aggregated projections of climate extremes," *Nature Climate Change*, vol. 3, no. 12, pp. 1033–1038, 2013.

[9] A. D. King, M. G. Donat, E. M. Fischer et al., "The timing of anthropogenic emergence in simulated climate extremes," *Environmental Research Letters*, vol. 10, no. 9, p. 094015, 2015.

[10] C. F. Schleussner, T. K. Lissner, E. M. Fischer et al., "Differential climate impacts for policy-relevant limits to global warming: the case of 1.5°C and 2°C," *Earth Syst. Dynam*, vol. 7, pp. 327–351, 2016.

[11] C. Mateus and A. Potito, "Long-term trends in daily extreme air temperature indices in Ireland from 1885 to 2018,"

Weather and Climate Extremes, vol. 36, Article ID 100464, 2022.

[12] G. F. Zebende, A. A. Brito, A. M. Silva Filho, and A. P. Castro, "pDCCA applied between air temperature and relative humidity: an hour/hour view," *Physica A: Statistical Mechanics and Its Applications*, vol. 494, pp. 17–26, 2018.

[13] S. H. Pour, A. K. A. Wahab, S. Shahid, and Z. B. Ismail, "Changes in reference evapotranspiration and its driving factors in peninsular Malaysia," *Atmospheric Research*, vol. 246, Article ID 105096, 2020.

[14] D. Wang, S. E. Giangrande, K. A. Schiro, M. P. Jensen, and R. A. Houze, "The characteristics of tropical and midlatitude mesoscale convective systems as revealed by radar wind profilers," *Journal of Geophysical Research: Atmospheres*, vol. 124, no. 8, pp. 4601–4619, 2019.

[15] K. Iizuka, K. Watanabe, T. Kato et al., "Visualizing the spatiotemporal trends of thermal characteristics in a peatland plantation forest in Indonesia: pilot test using unmanned aerial systems (UASs)," *Remote Sensing*, vol. 10, no. 9, p. 1345, 2018.

[16] I. T. Stewart, E. P. Maurer, K. Stahl, and K. Joseph, "Recent evidence for warmer and drier growing seasons in climate sensitive regions of Central America from multiple global datasets," *International Journal of Climatology*, vol. 42, no. 3, pp. 1399–1417, 2022.

[17] Y. Yan, D. Wang, S. Yue, and J. Qu, "Trends in summer air temperature and vapor pressure and their impacts on thermal comfort in China," *Theoretical and Applied Climatology*, vol. 138, no. 3–4, pp. 1445–1456, 2019.

[18] A. Hadri, M. E. M. Saidi, T. Saouabe, and A. El Alaoui El Fels, "Temporal trends in extreme temperature and precipitation events in an arid area: case of chichaoua mejjate region (Morocco)," *Journal of Water and Climate Change*, vol. 12, no. 3, pp. 895–915, 2021.

[19] M. F. Dreccer, J. Fainges, J. Whish, F. C. Ogbonnaya, and V. O. Sadras, "Comparison of sensitive stages of wheat, barley, canola, chickpea and field pea to temperature and water stress across Australia," *Agricultural and Forest Meteorology*, vol. 248, pp. 275–294, 2018.

[20] M. S. Kukal and S. Irmak, "Climate-driven crop yield and yield variability and climate change impacts on the U.S. Great plains agricultural production," *Scientific Reports*, vol. 8, no. 1, pp. 3450–3518, 2018.

[21] Ipcc, *Climate Change 2014 Synthesis Report Contribution of Working Groups I, II and III to the Fifth Assessment Report of the Intergovernmental Panel on Climate Change*, R. K. Pachauri and L. A. Meyer, Eds., IPCC, Geneva, Switzerland, 2014.

[22] J. D. S. Silva, J. B. Cabral Júnior, D. T. Rodrigues, and F. D. D. S. Silva, "Climatology and significant trends in air temperature in Alagoas, Northeast Brazil," *Theoretical and Applied Climatology*, vol. 151, no. 3–4, pp. 1805–1824, 2023.

[23] L. A. Vincent, X. Zhang, R. D. Brown et al., "Observed trends in Canada's climate and influence of low-frequency variability modes," *Journal of Climate*, vol. 28, no. 11, pp. 4545–4560, 2015.

[24] B. O. Ayugi and G. Tan, "Recent trends of surface air temperatures over Kenya from 1971 to 2010," *Meteorology and Atmospheric Physics*, vol. 131, no. 5, pp. 1401–1413, 2019.

[25] O. A. Anisimov and E. L. Zhil'tsova, "Climate change estimates for the regions of Russia in the 20th century and in the beginning of the 21st century based on the observational data," *Russian Meteorology and Hydrology*, vol. 37, no. 6, pp. 421–429, 2012.

[26] M. Higashino and H. G. Stefan, "Trends and correlations in recent air temperature and precipitation observations across Japan (1906–2005)," *Theoretical and Applied Climatology*, vol. 140, no. 1–2, pp. 517–531, 2020.

[27] S. H. Gebrechorkos, S. Hülsmann, and C. Bernhofer, "Long-term trends in rainfall and temperature using high-resolution climate datasets in East Africa," *Scientific Reports*, vol. 9, no. 1, pp. 11376–11379, 2019.

[28] O. W. Ilori and V. O. Ajayi, "Change detection and trend analysis of future temperature and rainfall over West Africa," *Earth Syst. Environ*, vol. 4, no. 3, pp. 493–512, 2020.

[29] K. Djaman, K. Koudahe, A. Bodian, L. Diop, and P. M. Ndiaye, "Long-term trend analysis in annual and seasonal precipitation, maximum and minimum temperatures in the southwest United States," *Climate*, vol. 8, no. 12, p. 142, 2020.

[30] S. Thakuri, S. Dahal, D. Shrestha et al., "Elevation-dependent warming of maximum air temperature in Nepal during 1976–2015," *Atmospheric Research*, vol. 228, no. June, pp. 261–269, 2019.

[31] D. Schaefer and M. Domroes, "Recent climate change in Japan- spatial and temporal characteristics of trends of temperature," *Climate of the Past*, vol. 5, no. 1, pp. 13–19, 2009.

[32] T. Caloiero, "Analysis of rainfall trend in New Zealand," *Environmental Earth Sciences*, vol. 73, no. 10, pp. 6297–6310, 2015.

[33] K. Chaouche et al., "Analyses of precipitation, temperature and evapotranspiration in a French Mediterranean region in the context of climate change," *Comptes Rendus Geoscience*, vol. 342, no. 3, pp. 234–243, 2010.

[34] S. del Río, L. Herrero, C. Pinto-Gomes, and A. Penas, "Spatial analysis of mean temperature trends in Spain over the period 1961-2006," *Global and Planetary Change*, vol. 78, no. 1–2, pp. 65–75, 2011.

[35] J. C. Gonzalez-Hidalgo, D. Peña-Angulo, M. Brunetti, and N. Cortesi, "Recent trend in temperature evolution in Spanish mainland (1951–2010): from warming to hiatus," *International Journal of Climatology*, vol. 36, no. 6, pp. 2405–2416, 2016.

[36] E. Yılmaz, "Monthly temperature, temperature difference trends and trends groups in Turkey<p>Türkiye'de aylık sıcaklık ve aylık ıcaklık farklarındaki eğilimler ve sıcaklık eğilim grupları," *Journal of Human Sciences*, vol. 16, no. 2, p. 392, 2019.

[37] M. Brunetti, M. Maugeri, F. Monti, and T. Nanni, "Temperature and precipitation variability in Italy in the last two centuries from homogenised instrumental time series," *International Journal of Climatology*, vol. 26, no. 3, pp. 345–381, 2006.

[38] N. Kalamaras, C. G. Tzanis, D. Deligiorgi, K. Philippopoulos, and I. Koutsogiannis, "Distribution of air temperature multifractal characteristics over Greece," *Atmosphere*, vol. 10, no. 2, p. 45, 2019.

[39] B. Boudiaf, I. Dabanli, H. Boutaghane, and Z. Şen, "Temperature and precipitation risk assessment under climate change effect in northeast Algeria," *Earth Syst. Environ*, vol. 4, no. 1, pp. 1–14, 2020.

[40] D. Dong, G. Huang, X. Qu, W. Tao, and G. Fan, "Temperature trend–altitude relationship in China during 1963–2012," *Theoretical and Applied Climatology*, vol. 122, no. 1–2, pp. 285–294, 2015.

[41] O. Ruiz-Alvarez, V. P. Singh, J. Enciso-Medina, R. E. Ontiveros-Capurata, and C. A. C. dos Santos, "Observed

trends in daily temperature extreme indices in Aguascalientes, Mexico," *Theoretical and Applied Climatology*, vol. 142, no. 3–4, pp. 1425–1445, 2020.

[42] S. G. Meshram, E. Kahya, C. Meshram, M. A. Ghorbani, B. Ambade, and R. Mirabbasi, "Long-term temperature trend analysis associated with agriculture crops," *Theoretical and Applied Climatology*, vol. 140, no. 3–4, pp. 1139–1159, 2020.

[43] J. Schilling, K. P. Freier, E. Hertig, and J. Scheffran, "Climate change, vulnerability and adaptation in North Africa with focus on Morocco," *Agriculture, Ecosystems & Environment*, vol. 156, pp. 12–26, 2012.

[44] F. Driouech et al., "Evaluation d'impacts potentiels de changements climatiques sur l'hydrologie du bassin versant de la Moulouya au Maroc," *IAHS-AISH Publication*, vol. 340, no. January, pp. 561–567, 2010.

[45] K. Khomsi, G. Mahe, M. Sinan, and M. Snoussi, "Hydro-climatic variability in two Moroccan basins: comparative analysis of temperature, rainfall and runoff regimes," *IAHS-AISH Proc. Reports*, vol. 359, no. July, pp. 183–190, 2013.

[46] W. Zkhiri, Y. Tramblay, L. Hanich, L. Jarlan, and D. Ruelland, "Spatiotemporal characterization of current and future droughts in the High Atlas basins (Morocco)," *Theoretical and Applied Climatology*, vol. 135, no. 1–2, pp. 593–605, 2019.

[47] S. Filahi, Y. Tramblay, L. Mouhir, and E. P. Diaconescu, "Projected changes in temperature and precipitation indices in Morocco from high-resolution regional climate models," *International Journal of Climatology*, vol. 37, no. 14, pp. 4846–4863, 2017.

[48] E. Hertig and Y. Tramblay, "Regional downscaling of Mediterranean droughts under past and future climatic conditions," *Global and Planetary Change*, vol. 151, pp. 36–48, 2017.

[49] A. Marchane, Y. Tramblay, L. Hanich, D. Ruelland, and L. Jarlan, "Climate change impacts on surface water resources in the Rheraya catchment (High Atlas, Morocco)," *Hydrological Sciences Journal*, vol. 62, no. 6, pp. 979–995, 2017.

[50] K. Khomsi, G. Mahe, Y. Tramblay, M. Sinan, and M. Snoussi, "Regional impacts of global change: seasonal trends in extreme rainfall, run-off and temperature in two contrasting regions of Morocco," *Natural Hazards and Earth System Sciences*, vol. 16, no. 5, pp. 1079–1090, 2016.

[51] E. Bouras, L. Jarlan, S. Khabba et al., "Assessing the impact of global climate changes on irrigated wheat yields and water requirements in a semi-arid environment of Morocco," *Scientific Reports*, vol. 9, no. 1, pp. 19142–19214, 2019.

[52] S. Ouhamdouch and M. Bahir, "Climate change impact on future rainfall and temperature in semi-arid areas (Essaouira basin, Morocco)," *Environ. Process*, vol. 4, no. 4, pp. 975–990, 2017.

[53] Z. Zamrane, *Recherche D'indices de Variabilité Climatique Dans des Séries Hydroclimatiques au Maroc: identification, Positionnement Temporel, Tendances et Liens Avec les Fluctuations Climatiques: cas Des Grands Bassins de la Moulouya, du Sebou et du Tensift*, Ph.D. thesis, p. 197, Montpellier University, Montpellier, France, 2016.

[54] M. Amiri, A. Salem, and M. Ghzal, "Spatial-temporal water balance components estimation using integrated GIS-based wetspass-M model in Moulouya Basin, Morocco," *ISPRS International Journal of Geo-Information*, vol. 11, no. 2, p. 139, 2022.

[55] A. François, E. Gauché, and A. Génin, "L'adaptation des territoires aux changements climatiques dans l'Oriental marocain: La vulnérabilité entre action et perceptions," *VertigO Rev. Électronique Sci. Environ*, vol. 16, 2016.

[56] R. Addou, M. Hanchane, N. Y. Krakauer et al., "Wavelet analysis for studying rainfall variability and regionalizing data: an applied study of the Moulouya watershed in Morocco," *Applied Sciences*, vol. 13, no. 6, p. 3841, 2023.

[57] A. Sbai, O. Mouadili, M. Hlal et al., "Water erosion in the Moulouya watershed and its impact on dams' siltation (eastern Morocco)," *Proceedings of the International Association of Hydrological Sciences*, vol. 384, pp. 127–131, 2021.

[58] V. Tekken and J. P. Kropp, "Climate-driven or human-induced: indicating severe water scarcity in the Moulouya river basin (Morocco)," *Water*, vol. 4, pp. 959–982, 2012.

[59] K. Diani, H. Tabyaoui, I. Kacimi, F. El Hammichi, and C. Nakhcha, "Stream network modelling from aster GDEM using ArcHydro GIS: application to the upper Moulouya river basin (eastern, Morocco)," *Journal of Geoscience and Environment Protection*, vol. 05, no. 05, pp. 1–13, 2017.

[60] A. A. Argiriou, Z. Li, V. Armaos, A. Mamara, Y. Shi, and Z. Yan, "Homogenised monthly and daily temperature and precipitation time series in China and Greece since 1960," *Advances in Atmospheric Sciences*, vol. 40, no. 7, pp. 1326–1336, 2023.

[61] O. Skrynyk, V. Sidenko, E. Aguilar et al., "Data quality control and homogenization of daily precipitation and air temperature (mean, max and min) time series of Ukraine," *International Journal of Climatology*, vol. 43, no. 9, pp. 4166–4182, 2023.

[62] R. Kessabi, M. Hanchane, T. Caloiero, G. Pellicone, R. Addou, and N. Y. Krakauer, "Analyzing spatial trends of precipitation using gridded data in the fez-meknes region, Morocco," *Hydrology*, vol. 10, no. 2, p. 37, 2023.

[63] A. R. Radivojević, N. Martic-Bursac, M. Gocic et al., "Statistical analysis of temperature regime change on the example of Sokobanja basin in Eastern Serbia," *Thermal Science*, vol. 19, no. suppl. 2, pp. S323–S330, 2015.

[64] Y. Latif, M. Yaoming, and M. Yaseen, "Spatial analysis of precipitation time series over the Upper Indus Basin," *Theoretical and Applied Climatology*, vol. 131, no. 1–2, pp. 761–775, 2018.

[65] L. Emmanuel, N. R. Hounguè, C. A. Biaou, and D. F. Badou, "Statistical analysis of recent and future rainfall and temperature variability in the Mono River watershed (Benin, Togo)," *Climate*, vol. 7, no. 1, p. 8, 2019.

[66] S. Adarsh and M. Janga Reddy, "Trend analysis of rainfall in four meteorological subdivisions of southern India using nonparametric methods and discrete wavelet transforms," *International Journal of Climatology*, vol. 35, no. 6, pp. 1107–1124, 2015.

[67] F. Tosunoğlu, "Trend analysis of daily maximum rainfall series in çoruh basin, Turkey," *Journal of the Institute of Science and Technology*, vol. 7, no. 1, pp. 195–205, 2017.

[68] H. B. Mann, "Nonparametric tests against trend," *Econometrica*, vol. 13, no. 3, pp. 245–259, 1945.

[69] H. Hotelling and M. R. Pabst, "Rank correlation and tests of significance involving No assumption of normality," *The Annals of Mathematical Statistics*, vol. 7, no. 1, pp. 29–43, 1936.

[70] M. Gocic and S. Trajkovic, "Analysis of precipitation and drought data in Serbia over the period 1980-2010," *Journal of Hydrology*, vol. 494, pp. 32–42, 2013.

[71] V. D. Banda, R. B. Dzwairo, S. K. Singh, and T. Kanyerere, "Trend analysis of selected hydro-meteorological variables for the Rietspruit sub-basin, South Africa," *Journal of Water and Climate Change*, vol. 12, no. 7, pp. 3099–3123, 2021.

[72] E. M. Douglas, R. M. Vogel, and C. N. Kroll, "Trends in floods and low flows in the United States: impact of spatial correlation," *Journal of Hydrology*, vol. 240, no. 1–2, pp. 90–105, 2000.

[73] M. Sayemuzzaman, M. K. Jha, and A. Mekonnen, "Spatio-temporal long-term (1950–2009) temperature trend analysis in North Carolina, United States," *Theoretical and Applied Climatology*, vol. 120, no. 1–2, pp. 159–171, 2015.

[74] O. Kisi and M. Ay, "Comparison of Mann-Kendall and innovative trend method for water quality parameters of the Kizilirmak River, Turkey," *Journal of Hydrology*, vol. 513, pp. 362–375, 2014.

[75] P. K. Sen, "Estimates of the regression coefficient based on Kendall's tau," *Journal of the American Statistical Association*, vol. 63, no. 324, pp. 1379–1389, 1968.

[76] M. A. Rahman, L. Yunsheng, and N. Sultana, "Analysis and prediction of rainfall trends over Bangladesh using Mann–Kendall, Spearman's rho tests and ARIMA model," *Meteorology and Atmospheric Physics*, vol. 129, no. 4, pp. 409–424, 2017.

[77] G. L. Makokha and C. A. Shisanya, "Trends in mean annual minimum and maximum near surface temperature in nairobi city, Kenya," *Advances in Meteorology*, vol. 2010, pp. 1–6, 2010.

[78] Wmo, *On the Statistical Analysis of Series of Observations*, WMO, Geneva, 1990.

[79] Z. Şen, "Innovative trend analysis methodology," *Journal of Hydrologic Engineering*, vol. 17, no. 9, pp. 1042–1046, 2012.

[80] F. Serinaldi, F. Chebana, and C. G. Kilsby, "Dissecting innovative trend analysis," *Stochastic Environmental Research and Risk Assessment*, vol. 34, no. 5, pp. 733–754, 2020.

[81] R. Singh, S. Sah, B. Das, S. Potekar, A. Chaudhary, and H. Pathak, "Innovative trend analysis of spatio-temporal variations of rainfall in India during 1901–2019," *Theoretical and Applied Climatology*, vol. 145, no. 1–2, pp. 821–838, 2021.

[82] A. N. Pettitt, "A non-parametric approach to the change-point problem," *Applied Statistics*, vol. 28, no. 2, pp. 126–135, 1979.

[83] T. A. Buishand, "Some methods for testing the homogeneity of rainfall records," *Journal of Hydrology*, vol. 58, no. 1–2, pp. 11–27, 1982.

[84] J. von Neumann, "Distribution of the ratio of the mean square successive difference to the variance," *The Annals of Mathematical Statistics*, vol. 33, no. 3, pp. 1187–1192, 1941.

[85] U. Z. Ekoğlu, G. Aktürk, M. Kendall, and M. Kendall, "Homogeneity and trend analysis of temperature series in hirfanli dam basin," *Journal of nature and science*, vol. 11, no. 1, pp. 49–58, 2022.

[86] S. Swain, D. Dayal, A. Pandey, and S. K. Mishra, "Trend analysis of precipitation and temperature for bilaspur district, Chhattisgarh, India," *World Environmental and Water Resources Congress*, 2019.